be one of the nodal parameters and then can be easily satisfied in the usual manner.

Numerical Examples and Discussion

Using the present Galerkin finite element method, the critical loads for three cases of stability of uniform cantilever column subjected to tangential loads, namely: 1) a subtangential concentrated load P at the free end; 2) a uniformly distributed tangential load of intensity q_o per unit length; and 3) a triangularly varying distributed tangential load of intensity q, where $q = q_o(1-x)$ are obtained.

Table 1 gives the critical load parameter λ_{cr} for case (1), for various values of γ. For the sake of comparison, the results of Ref. 4 and Beck's[6] values for $\gamma = 1$ are included in this Table. The results indicate that the present results are very accurate even with a two element idealization of the column.

Table 1 Stability parameter λ_{cr} of a uniform cantilever column subjected to sub-tangential concentrated load at the free end

	Present Work		Ref. 4	
γ	1 element[a]	2 elements[b]	5 elements[c]	Beck's[6] value
0.7	16.79019	16.78750	16.80	...
0.8	17.59646	17.58923	17.60	...
0.9	18.68248	18.66848	18.68	...
1.0	20.07538	20.05102	20.07	20.05

[a] Order of the dynamical matrix 4. [b] Order of the dynamical matrix 8.
[c] Order of the dynamical matrix 10.

Table 2 gives the critical load parameter λ_{cr} for cases (2) and (3) for one and two element idealizations. The results of Ref. 2 are also included for comparison. It can be seen from Table 2 that there is a slight discrepancy between the present results and those of Ref. 2. Because of the high accuracy and rapid convergence of the present finite element, we believe that the results obtained by the present element are more accurate.

Table 2 Stability parameter λ_{cr} of a uniform cantilever column with distributed tangential load

No. of	Case 1		Case 2	
elements	Present work	Ref. 2	Present work	Ref. 2
1[a]	40.05385		150.90001	
2[b]	40.05376		150.64225	
		40.7		158.2

[a] Order of the dynamical matrix 4. [b] Order of the dynamical matrix 8.

Conclusions

A Galerkin finite element is developed and successfully applied for the stability analysis of uniform cantilever column subjected to three types of tangential loading conditions. The results indicate that the convergence is very rapid and accurate results can be obtained even with a two element idealization. It is worthwhile to apply the method to other problems of stability of nonconservative systems and test the reliability of the present Galerkin finite element method.

References

[1] Bolotin, V. V., *Nonconservative Problems of the Theory of Elasticity*, Pergamon Press, Oxford, 1963.

[2] Leipholtz, H., *Stability Theory*, Academic Press, New York, 1970.

[3] Barsoum, R. S., "Finite Element Method Applied to the Problem of Stability of a Non-Conservative System," *International Journal of Numerical Methods in Engineering*, Vol. 3, 1971, pp. 63–87.

[4] Kikuchi, F., "A Finite Element Method for Non-Self-Adjoint Problems," *International Journal of Numerical Methods in Engineering*, Vol. 6, 1973, pp. 39–54.

[5] Mikhlin, S. G., *Variational Methods in Mathematical Physics*, Pergamon Press, Oxford, 1964.

[6] Beck, M., "Die Knicklast des einseitig eingespannten, tangential gedruckten Stabes," *Zeitschrift fuer Angewandte Mathematik und Physik*, Vol. 3, 1952, pp. 225–228.

Radiation from an Array of Longitudinal Fins of Triangular Profile

N. M. SCHNURR*
Vanderbilt University, Nashville, Tenn.

Nomenclature

A_P = profile area
A_R = reference area, $\sigma\varepsilon r_i^3 T_b^3/\kappa$
κ = thermal conductivity
L = fin width
N = number of node points
Q = heat transfer per unit length of fin array
Q_1 = heat transfer per unit length of fin array from Ref. 3
r = radial distance
r_i = tube radius
r_o = radial distance to the fin tip
t = local fin thickness
t_i = thickness of fin at the root
t_o = thickness of fin at the tip
T = temperature
T_b = base temperature
ε = emissivity
σ = Stefan-Boltzmann constant

Dimensionless Parameters

$N_c = 2\sigma\varepsilon T_b^3 r_i^2/\kappa t_i$ (the conduction number)
N_f = the number of fins
$N_L = L/r_i$
$N_P = t_o/t_i$
$Q^* = Q/(2\pi r_i \sigma T_b^4)$

Introduction

HEAT rejection in space depends solely on thermal radiation. This has resulted in widespread interest in radiation from various kinds of fins and fin arrays. One problem of particular interest is the augmentation of heat transfer from the outside surface of a circular tube by the addition of fins.

The circular fin array has been analyzed by Sparrow et al.[1] for black fins of rectangular profile and by Schnurr and Cothran[2] for gray circular fins of triangular profile. The straight fin and tube array has been investigated by Karlekar and Chao.[3] Their analysis included fin to fin interactions but fin to base interactions were neglected. Their results should, therefore, be applied only to cases where the tube radius is much smaller than the fin width.

The purpose of the work reported here is to analyze the straight fin and tube array (Fig. 1) including the effects of both fin to fin and fin to base interactions and to present results which may be used to optimize the design with respect to weight.

Received October 4, 1974. The author gratefully acknowledges the support of the NASA-Marshall Space Flight Center in the early stages of this work and particularly the aid and encouragement of C. A. Cothran.

Index category: Radiation and Radiative Heat Transfer.

* Associate Professor, Department of Mechanical Engineering.

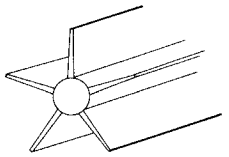

Fig. 1 Schematic of the physical system. Straight fin and tube array.

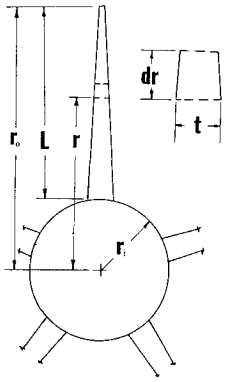

Fig. 2 Section of fin for analysis.

Analysis

A typical section of the system to be analyzed is shown in Fig. 2. The array consists of N_f fins of trapezoidal profile arranged symmetrically about the cylindrical base surface. The analysis is based on the following assumptions: 1) The fin thickness is very small compared to its width and to the axial length of the array so that the temperature distribution in the fin is one dimensional. 2) The cylindrical surface is isothermal. 3) All surfaces are radiatively gray and diffuse. 4) The thermal conductivity of the fin material is uniform. 5) There is no incident radiation from any source external to the system.

The determination of the temperature distribution in the fins requires the simultaneous solution of the differential equation for steady state conduction and the solution of the radiant heat transfer in a nonisothermal gray enclosure formed by two adjacent fins, the segment of tube surface between them and space. This solution is obtained by using a numerical method identical to that described in Ref. 2 with the exception of area and angle factor calculations. The independent dimensionless parameters which define the problem are the number of fins N_f, the emissivity of the surface ε, the conduction number $N_c = (2\sigma\varepsilon r_i^2 T_b^3)/\kappa t_i$, the geometric parameter $N_L = L/r_i$, and the profile parameter $N_P = t_o/t_i$. Results are presented in the form of a dimensionless heat transfer rate defined by $Q^+ = Q/(2\pi r_i \sigma T_b^4)$ where Q is the heat transfer rate from a unit length of fin array.

Results

The first series of runs was made to determine the effect of the base surface on the heat transfer from the fin array. A system having four fins of triangular profile was considered. The fin height L, base thickness t_i, base surface temperature T_b, and emissivity ε, were held constant while r_i was varied over a wide range. Results of these calculations are presented in Fig. 3. The abscissa is the ratio of heat transfer per unit length of fin array to that predicted by Karlekar and Chao[3] for an identical system of fins connected to a base cylinder whose radius is negligible compared to the fin width. Note that the heat transfer from an array having $r_i = 0.5L (N_L = 2)$ is twice as great as that from an array having identical fins but $r_i = (1/16)L$. Radiation from the base cylinder and the fin-base radiative interactions are significant up to $N_L = 8$. As N_L becomes very large the ratio Q/Q_1 approaches unity indicating good agreement with the results of Ref. 3.

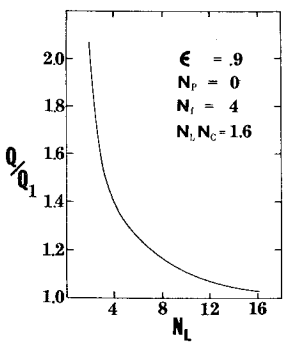

Fig. 3 The effect of the base cylinder on Q.

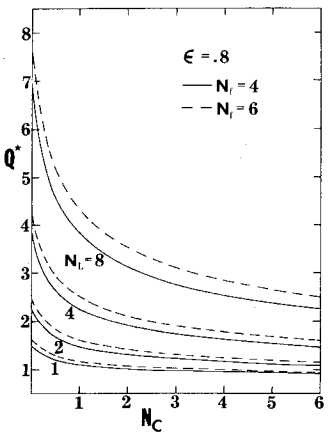

Fig. 4 Q^* vs N_c, $\varepsilon = 1.0$.

The effect of the fin profile on heat transfer was investigated by comparing cases for which N_P was varied from 0 (triangular) to 1 (rectangular) while all other parameters were held constant. It was found that the heat transfer from an array of fins having triangular profile was only 5 to 15% less than that from a comparable array having fins with rectangular profiles. Since the triangular profile gives a 50% weight saving, it is greatly superior from the standpoint of heat transfer per unit weight. Therefore all subsequent results presented here are for fins of triangular profile.

Finally, a parametric study was made to determine Q^* as a function of N_c, N_L, N_f, and ε. The ranges of those parameters considered were $\varepsilon = 0.8$–1.0, $N_c = 0$–6.4, $N_L = 2$–8, $N_f = 2$–16. Results are given in Figs. 4 and 5. The use of these results in designing a fin array for minimum weight proceeds as follows. Assuming the tube radius, surface temperature, emissivity and conductivity of the fin material, and the required heat transfer per unit length of tube are specified, the required value of Q^* may be calculated. Figs. 4 and 5 may then be used to determine N_c for any selected values of N_f and N_L. The conduction number may be written in the form

$$N_c = N_f N_L/(A_P/A_R)$$

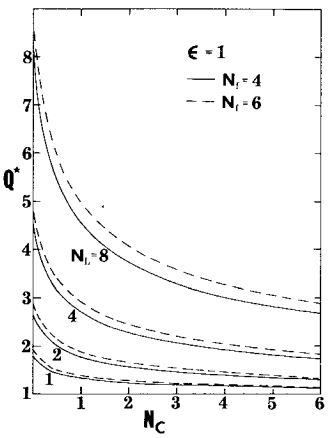

Fig. 5 Q^* vs N_c, $\varepsilon = 0.8$.

where $A_P = (1/2)t_i L N_f$ is the profile area and $A_R = \sigma \varepsilon r_i^3 T_b^3/\kappa$ is a reference area. Therefore (A_P/A_R) may be determined. The combination of N_f and N_L which gives the minimum value of A_P/A_R is the optimum design.

Several analyses of this type were carried out for various values of T_b, r_i, and Q to determine the ranges of parameters which might occur in optimally designed arrays. In all cases the optimum number of fins was found to be in the range $4 \leqq N_f \leqq 6$. Results are therefore given only for those values.

It should also be noted that the variation of heat transfer from the fin array with ε was found to be nearly linear in the range $0.8 \leqq \varepsilon \leqq 1.0$. Linear interpolation is therefore valid in this range.

Conclusions

Radiation from an array of longitudinal fins of triangular profile is analyzed including fin to fin and fin to base interactions. The effect of base cylinder radiation and the fin-base radiative interaction is found to be significant for N_L less than 8. The results presented here may be used to optimize the design of a fin array with respect to weight.

References

[1] Sparrow, E. M., Miller, G. B., and Jonsson, V. K., "Radiative Effectiveness of Annular Finned Space Radiators Including Mutual Irradiation Between Radiator Elements," *Journal of the Aerospace Sciences*, Vol. 29, 1962, pp. 1291–1299.

[2] Schnurr, N. M. and Cothran, C. A., "Radiation From an Array of Gray Circular Fins of Trapezoidal Profile," *AIAA Journal*, Vol. 12, Dec. 1974, pp. 1476–1480.

[3] Karlekar, B. V. and Chao, B. T., "Mass Minimization of Radiating Trapezoidal Fins with Negligible Base Cylinder Interaction," *International Journal of Heat Mass Transfer*, Vol. 6, 1963, pp. 33–48.

[4] Sparrow, E. M. and Cess, R. C., *Radiation Heat Transfer*, Brooks/Cole Publishing Co., Belmont, Calif., 1966, pp. 89–90.

Reverse Transition at an Expansion Corner in Supersonic Flow

R. NARASIMHA* AND P. R. VISWANATH†
Indian Institute of Science, Bangalore, India

Nomenclature

c_{f_o} = $\tau_o/\frac{1}{2}\gamma p_o M_o^2$
c_p = $(p_1 - p_o)/\frac{1}{2}\gamma p_o M_o^2 = -\Delta p/\frac{1}{2}\gamma p_o M_o^2$
L = length of boat-tail surface
M_o = freestream Mach number upstream of corner
p_o = freestream static pressure upstream of corner
p_1 = freestream static pressure just downstream of corner
R_o = Reynolds number per inch upstream of corner
R_{θ_o} = Reynolds number based on momentum thickness
τ_o = wall shear stress upstream of corner
δ_o = boundary-layer thickness upstream of corner
θ_o = momentum thickness upstream of corner
ε = expansion (or corner) angle in deg
γ = ratio of specific heats

I. Introduction

MANY investigators[1–7] have reported direct or indirect evidence indicating that in supersonic flow past an expansion corner the boundary layer reverts from a turbulent state upstream of the corner to a laminar state downstream. The present work is an attempt to identify a criterion for the occurrence of such reversion, in particular for use in calculations of base pressure[8] on boat-tailed bodies. At low speeds, highly accelerated turbulent boundary-layer flows have received considerable attention in recent years,[9–11] and different criteria for the occurrence of reversion, each often implicitly adopting a different means of recognizing the phenomenon, have been suggested. In particular, the theoretical work of Narasimha and Sreenivasan,[11] which employs the ratio of the pressure gradient to a characteristic Reynolds stress gradient as the parameter governing the completion of reversion, has been successful in correlating and predicting the flow development, particularly in the later stages of reversion. The basic idea in this study, namely that during reversion the Reynolds stresses have little influence in large parts of the flow, should be valid with even greater force in supersonic flow past an expansive corner. Indeed the parameter mentioned, namely the quantity $p'\delta/\tau_o$ (where p' is the pressure gradient, δ is the local boundary thickness, and τ_o is the wall shear stress in the boundary layer just upstream of the pressure gradient), takes on a simpler form in supersonic corner flow. For, the interaction of the expansion fan with the boundary layer spreads the pressure drop Δp (here considered positive in an expansion) over a few δ: the extent of this region appears to be insensitive to the total corner flow deflection, from Murthy and Hammitt's work.[4] Thus $-p' \sim \Delta p/\delta$, and consequently $-p'\delta/\tau_o \sim \Delta p/\tau_o$. This reasoning suggests that reversion will occur if $\Delta p/\tau_o$ is sufficiently large.

II. Data Analysis

To test this argument, we have examined all available experimental data (listed in Table 1 together with some relevant information), taking reversion to have occurred if there is evidence either of the growth of a thin new shear layer from the corner, or of a substantial change in the associated flow characteristics downstream (e.g., base pressure). This definition is appropriate to engineering calculations of recovery factor, skin friction, etc. Although it is not as precise as one might desire, nothing better is possible at present for supersonic flows, and the final results appear to justify it.

In the majority of the flows listed in Table 1 (the exception being Ref. 5), no value of τ_o is quoted, so we estimate it by the following procedure. First, it is assumed that the turbulent boundary layer upstream of the corner is fully developed and in equilibrium at constant pressure. Secondly, as all the experiments have been conducted under nearly adiabatic conditions, it is assumed that the skin friction coefficient just upstream of the corner, say c_{f_o}, depends only on the local Mach number M_o and Reynolds number R_{θ_o} (based on freestream conditions and momentum thickness θ_o). For this M_o and R_{θ_o}, c_{f_o} is obtained from the theoretical results of Tetervin.[12] (Over the range of M_o and R_{θ_o} covered in Table 1, a good fit to Tetervin's curves is given by

$$c_{f_o} = 0.0165\, M_o^{-0.36} R_{\theta_o}^{-0.20} \tag{1}$$

which is therefore a convenient expression for estimating τ_o.)

III. Classification of Data

The flows listed in Table 1 are plotted in Figs. 1 and 2 after classification into three categories. a) Those in which the authors themselves reported indications of reversion (shown by filled symbols in Figs. 1 and 2); b) Those in which reversion (in the sense described in Sec. II) is inferred here (shown by filled, flagged symbols); and c) Those in which no evidence of reversion can be found (shown by open symbols).

Each flow listed in Table 1 has been scrutinized in the light of the above classification in Ref. 13; only a brief outline of this examination is given. Group a consists of the experiments of Sternberg,[1] Vivekanandan[2] and Viswanath and Narasimha.[3] In Sternberg's experiments, reversion was indicated by recovery factor measurements, which dropped from the turbulent value upstream of the corner to the laminar value downstream.

Received October 8, 1974.
Index categories: Boundary-Layer Stability and Transition; Supersonic and Hypersonic Flow.

* Professor, Department of Aeronautical Engineering.
† UGC Research Fellow, Department of Aeronautical Engineering.